Electricity Generation from Natural Gas Solid Oxide Fuel Cell with Iron-Based Chemical Looping Combustion (NGSOFC-CLC) Technology: Process Modeling, Efficiency Analysis and Heat Integration

A Thesis

Presented in Partial Fulfillment of the Requirements for the Bachelor of Science Graduation with Honor Distinction in the College of the Engineering of The Ohio State University

By

Yu Gu

Department of Chemical and Biomolecular Engineering

The Ohio State University

2019

Undergraduate Thesis Committee

Andrew Tong, Advisor

Andrew Maxson

Abstract

With growing concerns of carbon emission from conventional fuel combustion power plants and increasing energy demand, it is necessary to optimize the power generation technologies. In recent years, the most dominant electric power generation method is the Natural gas combined cycle (NGCC) with downstream CO_2 compression system (CCS). However, the efficiency penalty resulted from a CO_2 separation process makes the NGCC less desired. Alternatively, due to the high efficiency and low environmental impact of Solid oxide fuel cell, many researchers study on Solid oxide fuel cell (SOFC) integration system, where fuel can be prepared via coal or biomass gasification process. Especially, the Solid oxide fuel cell/gas turbine cycle integrated with chemical looping hydrogen generation (CLHG-SOFC/GT) technology shows an efficiency of 43.53% without carbon emission, which is very attractive. However, due to the additional coal gasification unit and Air separation unit (ASU), the manufacturing could be capital-intensive. The natural gas chemical looping combustion shows a promising result in gas conversion, making integration of a Natural gas solid oxide fuel cell (NGSOFC) and a Chemical looping combustion (CLC) possible. The NGSOFC-CLC process is modeled with Aspen Plus (V10). The performance of the power plant is represented by Net power efficiency (NPE). There are various operating parameters could have an impact on the NPE. Especially, the parametric study of Fuel utilization (FU) factor shows that, within

an applicable range of FU factor values (0.75-0.90), with the increase of the FU factor value, the NPE increases and reaches a maximum at FU = 0.90. In addition, the Heat exchanger network (HEN) design base case is generated and studied by Aspen energy analyzer (AEA). Because the base case does not reach the target. An alternative design case is shown in this paper using pinch analysis method. Though the alternative design meets the energy goal, excessive heat exchangers are required. Also, the cross-sectional areas of heat exchangers are greater than that of the base case due to smaller approach temperature. Therefore, it is believed the base case design given by AEA is better.

Dedication

To the best mentor, Andrew Tong

Table of Contents

List of Tables

List of Figures

Abbreviations

NGCC	Natural gas combined cycle	NPE	Net power efficiency	CDR	Carbon dioxide recovery
CCS	CO_2 compression system	FU	Fuel utilization	LHV	Lower heating value
SOFC	Solid oxide fuel cell	HEN	Heat exchanger network	BG-SOFC	Biomass gasification-solid oxide fuel cell
CLHG-SOFC/GT	Solid oxide fuel cell/gas turbine cycle integrated with chemical looping hydrogen generation	AEA	Aspen Energy Analyzer	CHP	Combined heat and power
ASU	Air separation unit	EIA	Energy information administration	SOFC-CHP	Solid oxide fuel cell combined heat and power systems
NGSOFC	Natural gas solid oxide fuel cell	DOE	Department of energy	GT/ST	Gas turbine steam cycle
CLC	Chemical looping combustion	PC	Bituminous Coal	R-SOFC	Tubular internal reforming SOFC technology

NGSOFC-CLC	Natural gas solid oxide fuel cell (NGSOFC) and a chemical looping combustion	CTG	Combustion turbine generators	CFB	Circulating fluidized bed
				AU	Air utilization

Chapter 1. Introduction

It is generally accepted that energy is important for the development of society. As society developed, the demand for electricity increased sharply. According to the U.S. Energy information administration (EIA), the use of electricity is expected to grow steadily at around 1% growth rate through 2050 (EIA, EIA, 2018). It must be mentioned that electricity, is readily available and inexpensive due to its convenience in transferring energy and intensive penetration in the industry. It is an urgent need, but it is still a significant challenge to rationally produce electricity. With growing concerns about carbon emission from conventional power plants, it is important to innovate the electricity production sector to produce a more sustainable and economical electrical production process. In such a process, the carbon emission needs to be mitigated. The renewable energy-based power generation technologies are alternative methods to achieve the goal but due to the great demand for energy, the penetration into the market encountered some difficulties. (Nakata, 2010)

1.1 Literature Review

Electric power generation technology from NGCC

Traditional power generation via fossil combustion is still dominant in the industry. Currently, Natural Gas Combined Cycle (NGCC) is the most widely-applied method of electricity generation which accounted for 53% of the total U.S. natural gas-powered generator capacity. (EIA, 2017).

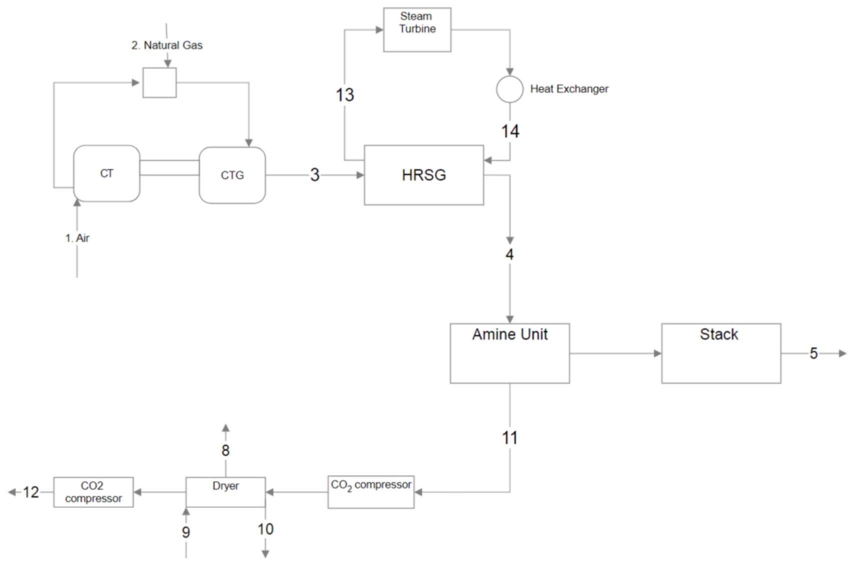

Figure 1: Block flow diagram of NGCC process

Figure 1 shows the NGCC case for electricity generation with 90% nominal CO_2 capture as analyzed in case B31B, in the U.S. Department of energy (DOE) report titled Cost and Performance Baseline for Fossil Energy Plants Volume 1a: Bituminous coal (PC) and Natural Gas to Electricity Revision 3. (Energy, 2015). NGCC is based on two Combustion turbine generators (CTG). During NGCC two different energy producing cycles are combined. In the first step, electricity is produced using two CTGs. A natural gas feed is reacted with compressed air at a high temperature in the reacting chamber of a combustion turbine to produce high temperature, high-pressure gas. The reaction is shown in Eq. (1).

$$CH_4 + O_2 \rightarrow CO_2 + H_2O \qquad \Delta\mathrm{H} = -802.3\ \mathrm{kJ/mole} \quad (1)$$

High energy gas goes through a set of turbine fan blades which spin the turbine shaft at high speed. The spinning shaft is directly attached to the generator which converts mechanical power to electricity. Each CTG used is typically supplied in full shop-fabricated modules that integrate mechanical, electrical, and control system required. The exhaust then is routed to the second electricity producing cycle Heat Recovery Steam Generator HRSG. HRSG is a specially designed boiler in nature. The hot exhaust transfer excess heat to water causing water to boil and convert to steam. The steam is then routed to a turbine that attached to an electricity generator to enlarge overall electricity generation. The NGCC case achieves 90% of the CO_2 capture by adding Carbon dioxide recovery (CDR) technology. A CDR facility used during NGCC purified the flue gas exiting HRSG and compressed it to a Standard critical SC condition. The CDR facility is based on the Cansolv system featuring an amine unit. The advantage of NGCC is higher net plant efficiency compared to a pulverized coal-fired power plant, which is the dominant approach to generate electricity (DOE, 2015). Since natural gas does not contain H_g, PM or HCl, the NGCC technology is environmental-friendly. However, the efficiency penalty resulted from carbon capture in NGCC is 11%, which results in an overall net plant efficiency of 50.6% with 90% CO_2 capture and in Lower heating value (LHV) basis. The normal range of penalty due to carbon capture process is around 8~12%. (report, 2010) So, it is necessary to develop the technologies of power generation using fossil fuel inefficient way with CO_2 capture. Some similar technologies' efficiencies are listed in Table 1.

Table 1: Coal-to Electricity Process Configurations and Process Efficiencies.

Process configuration	Conventional IGCC	CDCL-Combined Cycle	CDCL-SOFC
Efficiency (% HHV)	30-35	47-53	64-71
CO_2 capture rate (%)	90	100	100

Solid oxide fuel cell (SOFC) technology

Fuel cells are electrochemical devices that convert the chemical energy in fuels into electric energy directly, showing high efficiency and low environmental impact. Especially, the SOFC show that it is a promising technology for electric power generation. During SOFC, high operating temperature makes electrolyte, cathode, and anode oxygen ion-conductive. For example, the electrolyte used in NGSOFC is thin and full of dense oxygen ion O^{2-}. The dense electrolyte layer prevents natural gas (CH_4) from contacting air and burning. Each electrode is designed in high porosity to facilitate gaseous diffusion. As shown in Figure 2, the fuel source, CH_4 is directed to the anode/electrolyte interface and reacts with oxygen ions from electrolyte lattice. The overall reaction is:

$$CH_4 + 2O_2 \rightarrow CO_2 + 2H_2O \sim 8e^- \qquad (2)$$

The reaction taking place at the anode is shown in Eq. (3). Released electrons are transferred to the cathode through an external circuit. Compressed air flows across the cathode and reaches the electrolyte by pore diffusion. Electrons are thereby extracted from the cathode. The reaction occurred at the cathode is shown in Eq. (4) As discussed previously, high temperature is required to achieve SOFC electricity generation. SOFC operates at $600^{o}C \sim 1000^{o}C$, providing options for cogeneration applications in a SOFC system. (W. Zhang a, 2005) A well-integrated SOFC system is not only resulted from the high performance of the fuel cell unit itself but the optimal balance of the entire power plant.

$$CH_4 + 4O^{2-} \rightarrow CO_2 + 2H_2O + 8e^- \qquad (3)$$

$$2\,O_2 \;+ 8e^- \rightarrow 4O^{2-} \qquad (4)$$

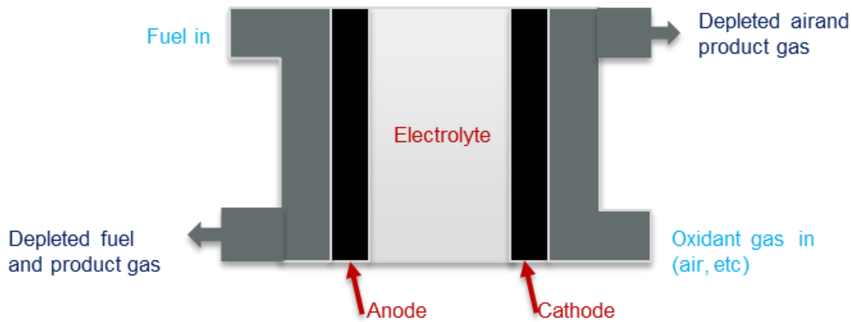

Figure 2: Configuration of a SOFC

Doherty et al. use biomass as a fuel source and studied the Biomass gasification-solid oxide fuel cell (BG-SOFC) combined heat and power (CHP) systems as shown in Figure 3. Aspen Plus (V10) is employed to simulate the entire process at a relatively small scale of 120 kW DC power output and shows an efficiency ranging from 66.8% to 71.2% with four varied operating conditions. (Doherty, Reynolds, & Kennedy, 2015) However, the application of SOFC-CHP is limited due to biomass logistics though the efficiency at small scale is high.

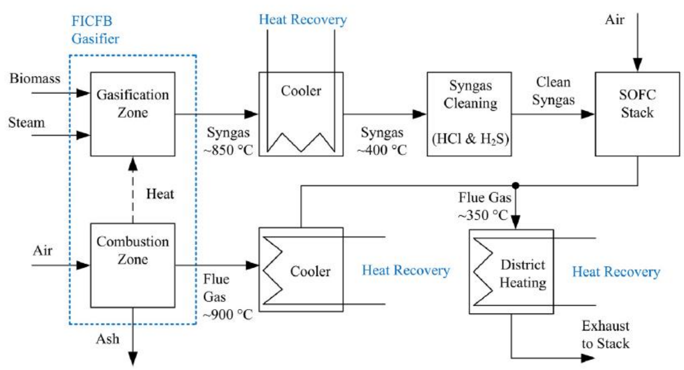

Figure 3: Simplified schematic diagram of a BG-SOFC CHP system

Chemical looping hydrogen generation integrated with SOFC/gas turbine cycle (CLHG-SOFC/GT) Technology

Chen et al. also designed a SOFC system: CLHG-SOFC/GT plant and modeled the process schematic Figure 3 using Aspen Plus (V10) software. The designed plant shows a net power efficiency of 43.53% with 100% CO_2 capture. Also, given that coal is the most abundant fossil fuels in the world, using coal as a fuel source is more attractive than biomass. To generate power, a gasification process to convert the coal to gaseous fuel before being fed to the SOFC unit is required. Syngas is produced by coal gasification process and is converted into H_2 and CO_2 through the three-reactor chemical looping hydrogen generation process (CLHG). After H_2 being utilized in SOFC unit, the unreacted H_2 is sent to the combustor where the released heat from combustion can drive the Gas turbine steam cycle (GT/ST). The CO_2 exhaust from oxidizer is sent to CO_2 compression system to be further processed.

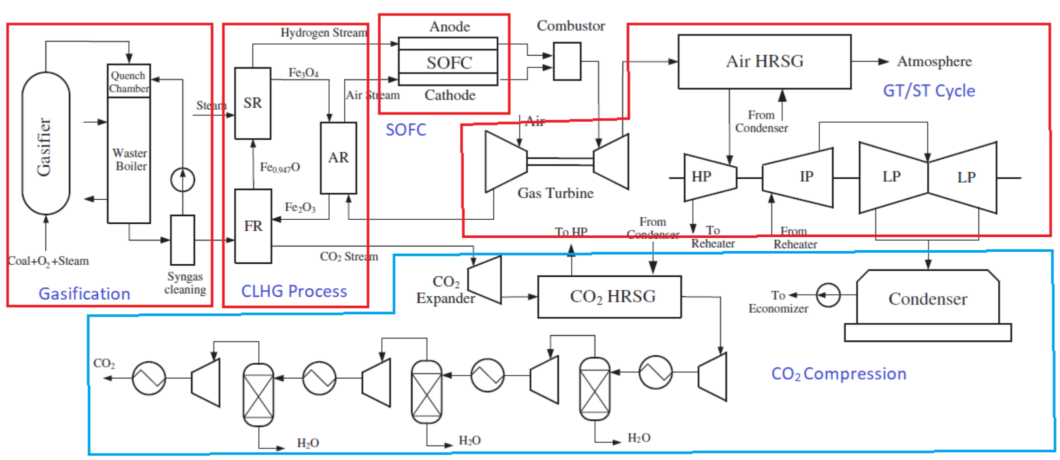

Figure 4: Schematic Layout of the CLHG-SOFC/GT hybrid plant integrated with coal gasification

Besides CLHG-SOFC/GT technology, there is extensive research on the integrated system of SOFC and gas turbine (SOFC/GT). Since natural gas is one of the most widely-used feedstocks of SOFC, under a high operating temperature of the SOFC unit, natural gas can be reformed to syngas in internal reformer and then be routed to SOFC reacting space. Yi et al. (Yaofan, Ashok, Jacob, & G. Scott, 2005)investigated several operating parameters and found the NPE under each specific parameter setting. This design features placing in-stack reformer sections between rows of bundles formed by an electrically interconnected single cell. The result shows that the system electrical efficiency is higher than 75% under high operating pressure and less excess air in SOFC unit.

Zhang et. al. designed a SOFC model based on the Tubular internal reforming SOFC technology (R-SOFC) developed by Siemens-Westinghouse. As shown in Figure 5, during the fuel supply system, the desulfurized natural gas is converted to syngas in a pre-reformer (“REFORMER” in the figure). Then, the reformed gas consisting of CO, H_2 and unreacted CH_4 entered the SOFC unit, where the further shifting reactions and reforming occur and produced more H_2. Meanwhile, electrochemical reaction Eq. (5) occurs as well. The Aspen Plus (V10) simulation result shows that the gross AC efficiency is 52% without CO_2 capture. Therefore, considering the potential efficiency penalty, the corrected NPE can be lower than 40% which is less desired.

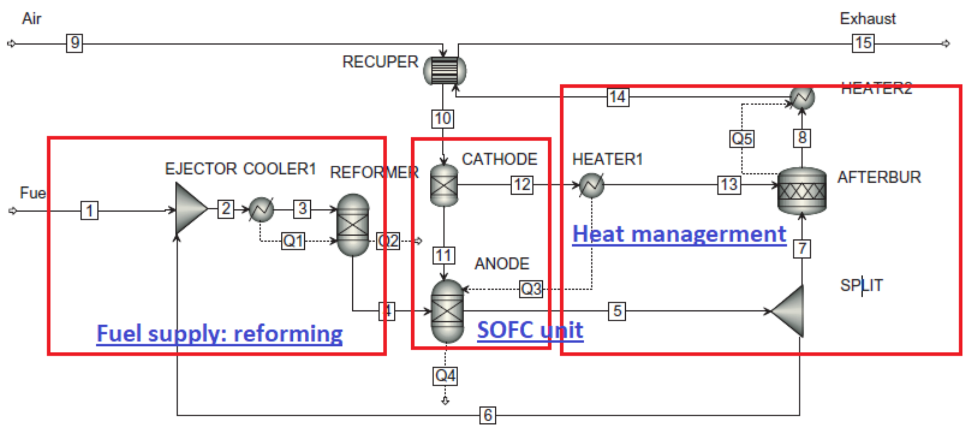

Figure 5: Aspen Plus SOFC model flowsheet

$$H_2 + \frac{1}{2}O_2 \rightarrow H_2O \qquad (5)$$

Summary

In summary, there are various technologies to generate electricity varied by fuel sources and basic principle. As the dominant technology to produce the electricity, NGCC plant with 90% CO_2 capture shows an NPE at 50.6% where 11% efficiency loss is due to the carbon capture process. Fuel cells are a promising power generation method with low environmental impact. Because usually in a fuel combustion-based power plant, the chemical energy is first converted into thermal energy, and then the heat is used to power the steam cycle to achieve energy transfer from heat to mechanical work. During the fuel cell, the chemical energy can be transferred into electrical energy directly without being limited by thermodynamic limitations of heat engines such as Carnot efficiency. (EG&G Technical Services, 2004) Furthermore, since the combustion process is avoided, the fuel cell reduces potential pollution caused by flue gas.

SOFC allows for power generation using a wide range of fuels like CO, H_2, and CH_4. Especially, the high operating temperature also provides the option for integration applications. For example, BG-SOFC-CHP uses biomass as fuel and generates electricity with efficiency above 66.8%. But due to fuel source limitations, more researchers turn to other options. CLHG-SOFC/GT realized 43.53% NPE with 90% carbon capture. This technology is attractive because of the abundance of coal. Instead of implementing the gasification unit at the upstream of the plant, the SOFC/GT and R-SOFC utilize natural gas as fuel, which simplifies the plant design. Both technologies convert CH_4 into syngas during the reformer first and then send the syngas to the SOFC unit finish the shifting step and electrochemical conversion. Considering the separation of CO_2 from cathode exiting mixture, the gross AC efficiency could be relatively low.

1.2 Project purpose

Like mentioned earlier, converting energy to products like electric power with high efficiency is a great challenge for any fossil fuel conversion system. CLHG-SOFC/GT provides an attractive option to generate electricity utilizing coal instead of CH4 as fuel because of the abundance of fuel source. Meanwhile, it also maximizes the NPE by combining GT/ST cycles to maximize heat recovery. However, in this power plant, the gasification unit makes the entire plant design complicated. Also, since an ASU is necessary for the industrial plant but not shown in Figure 4, the total cost will be increased. To achieve high overall efficiency, it is important to come up with a proper strategy. This paper provides such a strategy where electricity can be generated from NGSOFC-CLC process.

1.3 Project scope

The study focuses on process modeling, NPE analysis and the heat integration of this process using Aspen Plus (V10) and Aspen Energy Analyzer (AEA). There are three major systems in this design: CLC, SOFC, and heat recovery system. During each individual system, the parametric studies of varying operating parameters can be studied. But in this paper, only one factor: fuel utilization factor of SOFC unit is investigated in a selected range while keeping all other factors unchanged and then the energy analysis and heat integration with the built model is studied. The resulted NPEs will be taken to compare with NPE of CLHG-SOFC/GT technology by Yang et al.

The schematic diagram of the NGSOFC-CLC process is shown in Figure 6. There are two major sections in this process: NGSOFC unit, CLC process. The natural gas and air are pre-heated and sent to the anode and cathode respectively. The exit gas from the anode remains a great of amount of unreacted natural gas and the cathode exit gas is O_2 depleted air. The two streams enter reducer and combustor respectively. The reducer uses iron oxide as an oxygen carrier. An oxygen carrier can transfer oxygen from the air to the fuel without direct contact between fuel and combustion air. In this case, the dilution of CO_2 by N_2 is avoided. The gas exiting the fuel reactor is at high temperature and contains CO_2 and H_2O. Since the H_2O is easily condensed, CO_2 can be separated, compressed and stored for future usage.

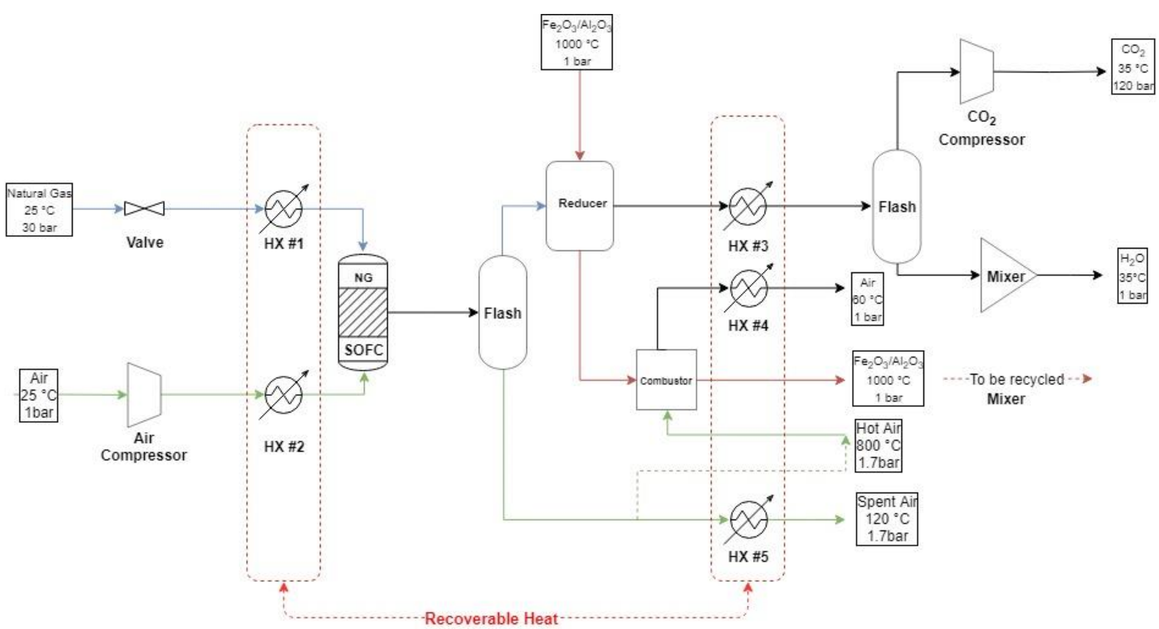

Figure 6: Schematic diagram of the NGSOFC-CLC process

2.1 SOFC

Generally, the electrical efficiency is a function of voltage, current density, temperature, pressure, and composition of the fuel. (EG&G Technical Services, 2004) In an actual cell, the output voltage is lower than the ideal value due to polarization, ohmic loss, and concentration polarization. In this paper, the stack performance is not considered but a single SOFC unit is taken into discussion. The voltage output can be calculated with the Nernst Equation as shown in Eq. (6). The reference cell voltage at the operating temperature needs to be corrected once the operating conditions are changed from standard condition (molar concentration is no longer 1.0 and/or pressure is not 1 atm). The change is represented by ΔV. Q is the reaction quotient and can be calculated as shown in Eq. (7). The reference value adopted V_{ref} is at 800 C standard conditions, 1.037 V; R is the universal gas constant, 8.31 J / (mol*K); T is the SOFC operating temperature, 1073.15K (800 C) in this paper; n is the number of electrons transferred per reaction, which is e^{-}. F is the Faraday constant 96485 J/(mol*V);

$$V = V_{ref} + \Delta V = V_{ref} + \frac{RT}{nF}\ln Q \quad (6)$$

$$Q = \frac{[CO_2][H_2O]^2}{[CH_4][O_2]^2} \quad (7)$$

The direct current (DC) power output $W_{SOFC*DC}$ can be calculated as shown in Eq. (8). n_{CH_4} is the consumed CH4 mole flowrate. The efficiency of DC-AC inverter is assumed to be at 95% so the AC power output can be calculated as shown in Eq. (9). The FU value setting in SOFC block in Aspen Plus (V10) is achieved by *INERT* function in a RGIBBS reactor.

$$W_{SOFC*DC} = V * I = V * \left(n_{CH_4} * nF\right) \qquad (8)$$

$$W_{SOFC*AC} = W_{SOFC*DC} * \eta_{DC-AC} \qquad (9)$$

2.2 CLC process

Reducer (fuel reactor)

The reducer employed in the CLC process is a counter-current moving bed. Iron oxide (Fe2O3) entered the reactor on the top and goes downward. The natural gas is injected at the bottom and goes upward. The chemical reaction taking place in the reducer is shown in Eq. (10). The natural gas is completely oxidized to CO_2 and H_2O while Fe_2O_3 is reduced to lower oxidation state resulted in a mixture of Fe_3O_4, FeO and Fe. Since the reaction is endothermic and the reactor is adiabatic, it will cause a temperature drop. To mitigate the temperature drop, the supporting materials like Al_2O_3 can be added to Fe_2O_3 to form an oxygen carrier compound.

$$CH_4 + \left(\frac{4}{3-2x}\right) Fe_2O_3 \rightarrow CO_2 + 2\ H_2O + \left(\frac{8}{3-2x}\right) FeO_x,\ (0 < x < 1.5) \qquad (10)$$

A key issue in CLC considerations is the type of reactor chosen. The Circulating fluidized bed (CFB) is considered as the most promising set-up for the reliable and consecutive operation of the CLC process. (Tobias Mattisson) However, since a moving bed reactor has less axial mixing of the gas and solid, especially, in a counter-current moving bed, the fresh syngas can contact iron oxide at lower oxidation state. From thermodynamics of this component system, this contacting pattern will maximize the solids and gas conversions. (Fan, 2011) the solids conversion is defined as in Eq. (11). $\frac{n_O}{n_{Fe}}$ corresponds to the molar ratio between the oxygen atom and the iron atom in Fe_2O_3, and $\hat{n}_O/\hat{n}_{Fe}$ corresponds the molar ratio between the oxygen atom and the iron atom in the oxidized solid product, FeO_x ($1<x<\frac{4}{3}$).

$$y = \frac{\frac{n_O}{n_{Fe}} - \frac{\hat{n}_O}{\hat{n}_{Fe}}}{\frac{n_O}{n_{Fe}}} \times 100\% \qquad (11)$$

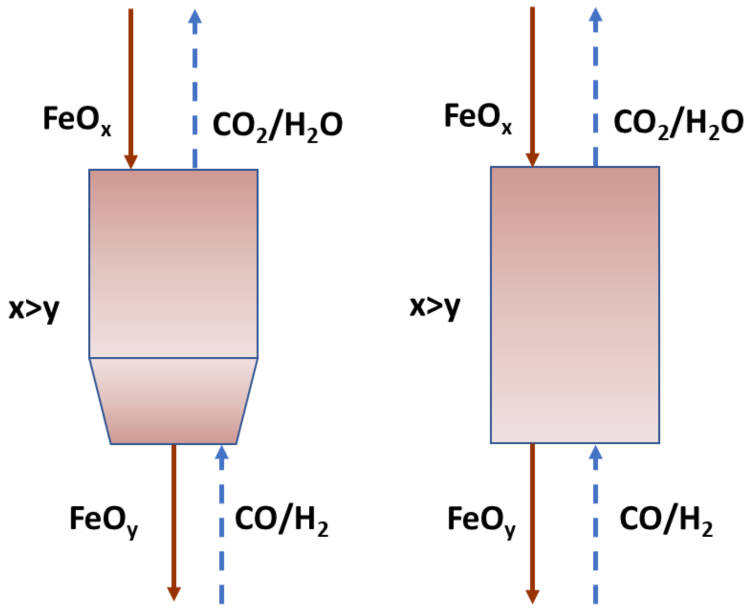

Figure 7: Gas-solid contacting pattern of the reducer: a fluidized bed vs. a moving bed

Combustor (air reactor)

The reaction taking place at the combustor is shown in Eq. (12). Since the oxidation reaction is exothermic, it is relatively fast and thermodynamically favored. Therefore, the combustor can fully oxidize the oxygen carrier exit from the bottom of the reducer to its highest oxidation state. In this case, due to significant mixing of the gas and the solids in a fluidized bed, the fluidized bed is chosen as the design for the combustor. The combustion air can use depleted cathode exit gas which remains a great amount of O2 and at high temperature.

$$\left(\frac{4}{3-2y}\right)FeO_y + O_2 \rightarrow \left(\frac{2}{3-2y}\right)Fe_2O_3 \qquad (12)$$

2.3 Process Simulation and Design Specification

The characteristics of each plant component are implemented in Aspen Plus (V10) using built-in functions and modules. The actual Aspen Plus (V10) simulation flowsheet is shown in Figure 8. All functioning unit is included in the flowsheet: conditioning of the fuel and air, the SOFC unit, the reducer reactor, combustor, CO_2 compression system and heat exchangers. In the following sections, terms in italics represent terminology in Aspen Plus (V10).

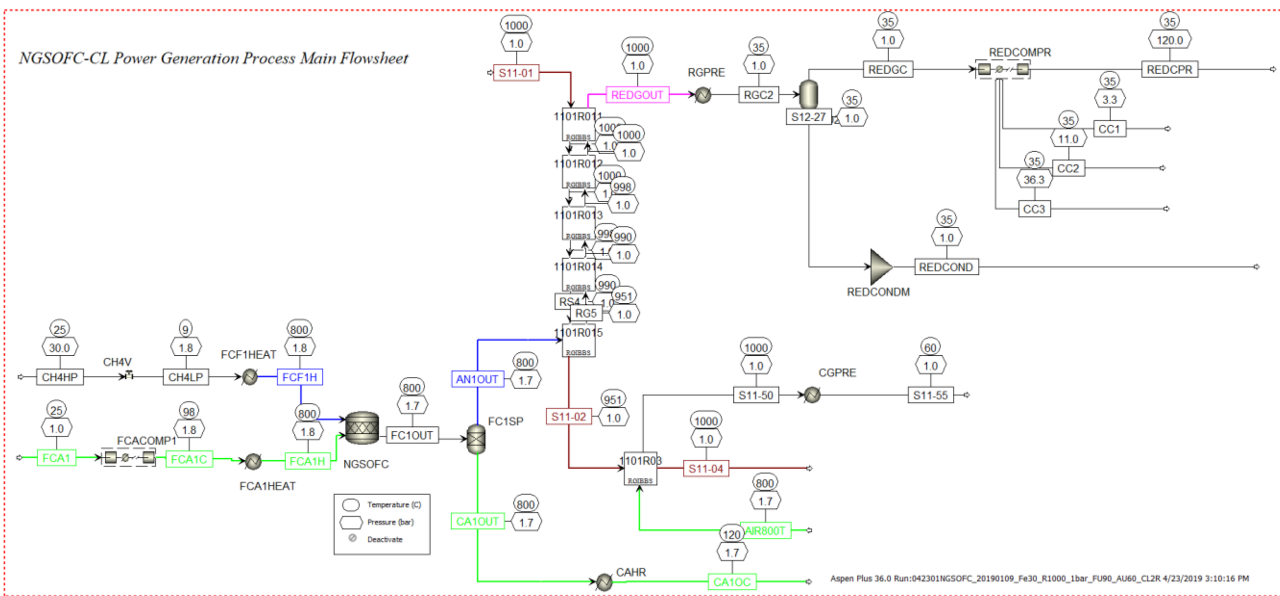

Figure 8: Aspen Plus NGSOFC-CLC model flowsheet.

Aspen simulation model set-up

The simulation model is constructed under some global settings, which is shown in Table 1. The used chemical components are shown in Table 2. As mentioned in the earlier chapter, the reducer of the CLC process is a counter-current moving bed and the combustor is a fluidized bed. Based on several case studies, it shows that the counter-current moving bed can be simulated by a five-stage RGIBBS configuration as shown in Figure 9 and the fluidized bed can be modeled by a single stage RGIBBS block. (Fan, 2011) One of the most attractive benefits of RGIBBS is that there exists a built-in module in Aspen Plus RGIBBS block to determine the equilibrium condition in the reacting system. (Fan, 2011) The oxygen carrier used in this simulation is made up of Fe_2O_3 and Al_2O_3 in a weight % ratio of 30%: 70%. The flow rate of fuel is adjusted to 1 kmol/hr to facilitate the calculation. The fuel utilization (FU) factor is adjusted from 0.75 to 0.95. Based on electrochemical reaction occurred in the SOFC and chosen FU and Air utilization (AU) factor value, the air flow rate can be calculated. The natural gas used in this case is assumed to be 100% CH_4.

Table 2: Model basic set-up

Global unit set	METBAR
Input mode	Steady-state
Stream class	MIXCISLD
Flow basis	MASS
Ambient pressure and temperature	1.01325 bar, 10 °C

Thermodynamic and physical data bank	Combust, Inorganic, Solids, Aqueous, Pure 36

Table 3: Chemical components list

Solids	Fe_2O_3; Fe_3O_4; $Fe_{0.947}O$; Fe; Al_2O_3
Liquids and gas	CO; CO_2; H_2; H_2O; CH_4; N_2; C_2H_6; C_3H_8; C_4H_{10}; O_2 ; NO; NO_2;

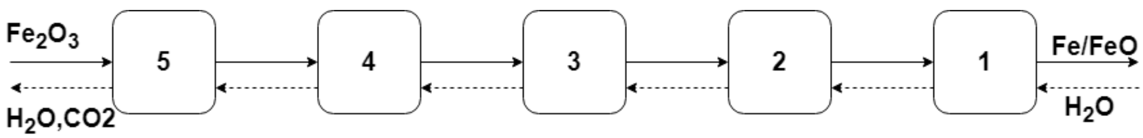

Figure 9: Aspen Plus (V10) simulation of a five-stage RGIBBS model for reducer reactor in the process

Overall heat integration

As shown in process flowsheet Figure 6, there are five heat exchangers used in the plant. The pre-heater HX#1 *"FCF1HEAT*" and HX#2 "*FCA1HEAT*" for fresh CH4 and air. The cooling device HX#3 "", HX#4 "" and HX#5 "" for cooling down reducer exit CO_2 and steam, the depleted air (mainly N_2) from combustor and cathode exit gas (mainly N_2 and a trace amount of O_2 and H_2O). Besides that, the NGSOFC is operated isothermally so there is one cold utility required as well to maintain the operating temperature of the fuel cell. The CO_2 compression system is modeled by a multi-stage isentropic compressor where 4 stages are used with four liquid knockout streams. The compression ratio is 3.5 and this is based on value recommended in the DOE report. (Energy, 2015) The interstage cooling temperature is set at 35 °C. One of the benefits of using Aspen Plus (V10) is that the heat exchanger network (HEN) design of the NGSOFC-GT process can be provided by Aspen Energy Analyzer. Besides the HEN design generated by AEA, an alternative HEN design emphasizing the internal heat exchange is demonstrated in this paper via pinch analysis. During the analysis, the trade-off between operating cost and the total utility is considered. Since this paper focuses on discussing NPE, the pinch temperature is set as 10 °C to minimize the external utility usage though this causes larger heat-exchanger areas. Finally, an energy saving summary can be drawn to compare target total utilities, actual utilities given by AEA and by manual pinch analysis. The detailed discussions can be found in the later chapter. The complete assumptions adopted in this simulation is shown in Table 3.

Table 4: List of assumptions of the simulation model set-up

Main design assumptions adopted in the simulation	
Parameters	Specifications
Solid oxide fuel cell	
Operating temperature	800 °C
Operating pressure	1.8 bar
Fuel utilization factor	0.75-0.95 with an increment of 0.05
Air utilization factor	0.6
DC-AC inverter efficiency	90%
Side-reaction	No
Natural gas chemical looping	
Oxygen carrier	Fe_2O_3 supported by inert Al_2O_3 (Al_2O_3 wt ratio 0.7)
Reducer outlet temperature	≥750 °C
Reducer outlet solid conversion	≤65%
Reducer pressure drop	0 bar
Air and CO_2 compression	
Air compression # of stage(s)	Single stage
CO_2 compression # of stages	4
Air/CO_2 Compression ratio	3.5,
Air compression efficiency	100%
CO_2 compression efficiency	60%
Heat recovery steam generation	
Approach temperature difference, ΔT	10 °C
ST/GT cycle efficiency	48%
Pinch point	800 °C

Plant performance analysis

In this paper, the most important parameter is the Net power efficiency (NPE), which is defined in Eq (13). W_{net} is the net power of the entire plant, kW; n_{NG} is natural gas mole flowrate, kJ/hr; HHV_{NG} is the natural gas higher heating value (HHV), kJ/mol. The net power of the plant W_{net} is calculated according to Eq (14). The power generation is denoted by "+" and power consumption is denoted by "- ". $W_{SOFC*AC}$ is the SOFC output AC power, kW; $W_{air*comp}$ and $W_{CO2*comp}$ is the compressor power of air and CO2 in kW, respectively; $W_{HB/ST}$ is the power can be generated from steam turbine if the heat balance is considered and the recovered heat is used for electricity generation from steam turbine cycle. $W_{HB/ST}$ is calculated according to Eq (15). η_{ST} is the efficiency of the steam turbine cycle, 48%. $Q_{preheat}$ is the heat required to heat up the fresh air and natural gas, kW; $Q_{red*out}$, Q_{comb}, $Q_{cathode}$ are the heat duties of the HX #3, HX#4 and HX#5, respectively in the unit of kW. The NPE of the CLHG-SOFC/GT process, which is 43.54% will be used for comparison purpose.

$$NPE = \frac{W_{net}}{n_{NG} * HHV_{NG}} \quad (13)$$

$$W_{net} = W_{SOFC*AC} - W_{air*comp} - W_{CO2*comp} + W_{HB/ST} \quad (14)$$

$$W_{HB/ST} = \eta_{ST} * (Q_{preheat} + Q_{red*out} + Q_{comb} + Q_{cathode}) \quad (15)$$

Chapter 3. Results and Discussion

3.1 Parametric study on fuel utilization (FU) factor and Plant performance

There are several operating parameters can impact the performance of the power plant. For fuel supply steps: the fuel composition. For SOFC unit: the fuel composition, fuel utilization factor, the air utilization factor, the current density, and power output. For the CLC system: the solids composition (inert materials weight percentage), solids inlet temperature and pressure. This paper will use the FU factor as an example to show how to study each individual parameter affects the NPE.

Sensitivity analysis can help to understand the effects of varying operating parameters on the SOFC unit's performance, and on downstream units' performance. This benefit is more significant when there are numerous parameters to be studied. However, since there is only one parameter of interest in this study, instead of setting up the sensitivity analysis module, the relationship between the examined parameter FU and the plant NPE can be found by running the simulation one by one and recording the generated results. This can be achieved by: first, create a *CALCULATOR* excel space, import all necessary variables /parameters and create characteristic variables that can be used to calculate the NPE; Second, go back to flowsheet SOFC module and assign a value to FU variable while keeping all other parameters unchanged; Third, run the simulation and find results of NPE in excel space.

The FU factor is one of the most important parameters in cell design. It represents the amount of fuel reacted in the cell divided by the total inlet fuel. In this paper, the fuel utilization varying range is between 0.75 to 0.95 with a 0.05 increment based on range chosen by (Shiyi Chen, 2012) and (EG&G Technical Services, 2004). Ideally, the FU factor can be any value between 0 to 1. But FU value usually cannot reach 0.90 due to kinetics limit. (Shiyi Chen, 2012). In this paper, though the FU value 0.95 is still considered, from the results, we can find the NPE is decreasing when FU > 0.90. The values below the 0.75 are also not applicable because too much unreacted natural gas might cause over-heating of the reducer.

It is suggested in Figure 10 that with the increase of the FU factor, the NPE increase from 0.75 to 0.90. The fuel utilization has a direct impact on cell voltage as suggested in Figure 11.

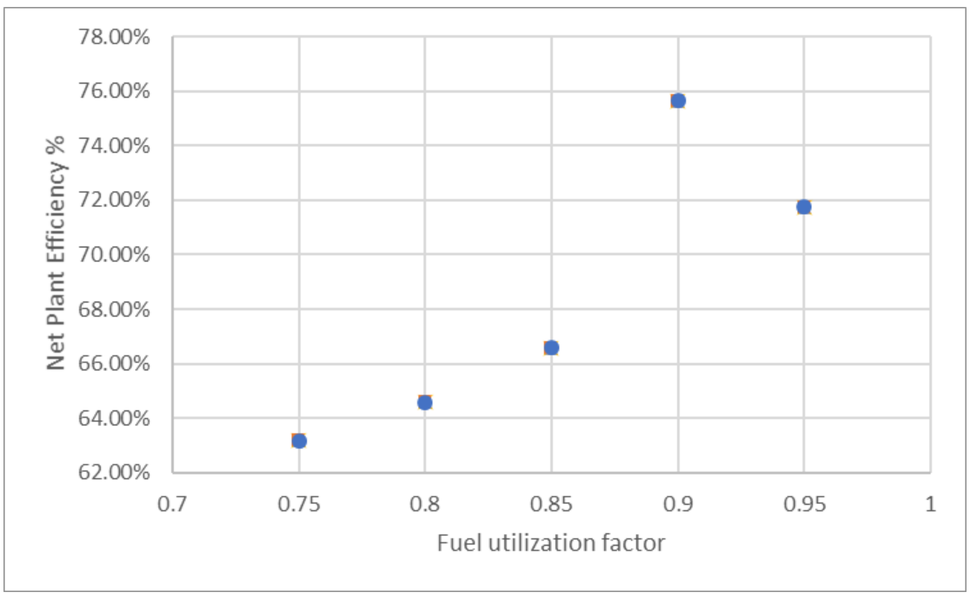

Figure 10: NPE vs. FU factor

As more fuel is utilized in the fuel cell, the less the cell voltage will be. Since in the test range of FU factor values, the quotient of the reaction is less than 1, resulting in the negative voltage change ΔV from the reference voltage. As more CH_4 consumed, the concentration of CH_4 in the outlet stream is less, resulting in a larger ΔV decrease. Therefore, the actual voltage output is less.

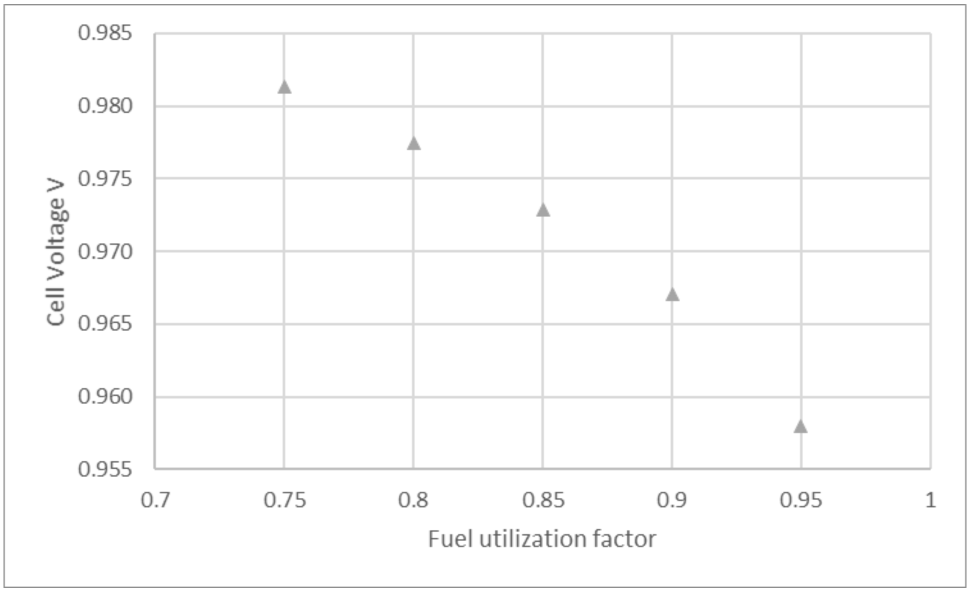

Figure 11: Cell voltage vs. FU factor

As shown in previous gross power $W_{SOFC*DC}$ calculation Eq. 42, as FU factor increases, n_{CH_4} increases and the actual cell voltage decreases. From Figure 12, it is suggested that fuel consumption has a greater impact on gross power than cell voltage because the overall trend is increasing.

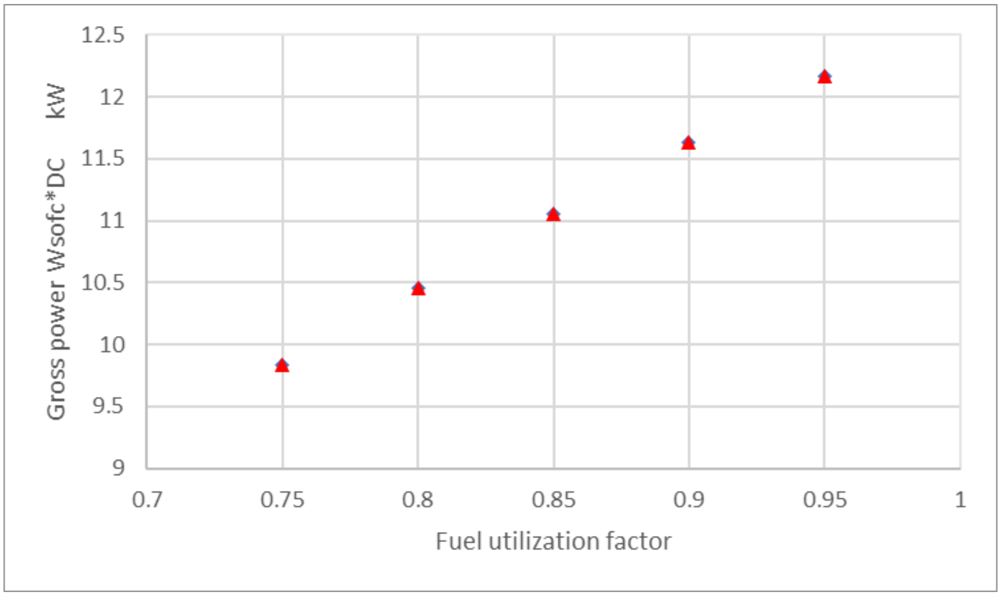

Figure 12: Gross power $W_{SOFC*DC}$ vs. FU factor

At a higher FU factor whiling keeping all other operating parameters of the CLC process unchanged, less natural gas enters the fuel reactor. Given that the solids inlet condition stays the same, the temperature of the reducer exit gas and reducer exit solids are lower than before. The heat duties of the HX #3 and HX#4 are lower, resulting in a less Q_{net} value and a less W_{aux} value.

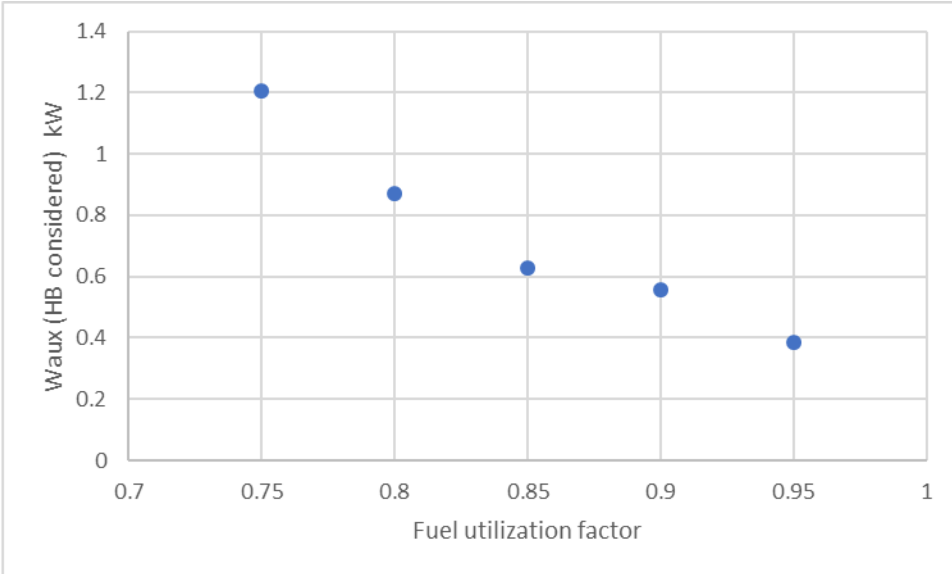

Figure 13: Q_{net} vs. FU factor

From the equation to calculate the NPE, it is obvious that the total thermal energy of fuel CH (Energy, 2015) in HHV, the compression work of air $W_{air*comp}$ and the compression work of CO_2 $W_{CO2*comp}$ are the same as FU factor increases. When the FU increases, the NPE increases, which means the increase of $W_{SOFC*DC}$ has a more significant effect on it than the decrease of the work generated by recovered heat. Especially, the optimal plant performance is achieved at an FU of 0.9. Under this operating condition, the NPE is 75.65%, which is higher than the CLHG-SOFC/GT case. The more detailed impact of FU factor on other parameters is shown in Table 4.

Table 5: Plant performance vs. FU factor

Fuel utilization	unitless	0.75	0.8	0.85	0.9	0.95
Air utilization	unitless	0.6	0.6	0.6	0.6	0.6
Net eff	%	55.33%	58.92%	62.50%	72.03%	69.25%
Cell voltage	V	0.98	0.98	0.97	0.97	0.96
dH base FC eff	%	94.58%	94.20%	93.76%	93.20%	92.33%
fuel HHV FC eff	%	85.20%	84.86%	84.47%	83.96%	83.18%
Total thermal	kW	15.39	15.39	15.39	15.39	15.39
preheat req	kW	5.46	5.78	6.09	6.40	6.72
heat balance	kW	-2.52	-1.82	-1.31	-1.16	-0.80
Fuel cell air in	kmol/hr	0.76	0.86	0.86	0.91	0.96
Fuel cell air out	kmol/hr	0.67	0.76	0.76	0.80	0.84
Combustor air in	kmol/hr	0.27	0.14	0.14	0.14	0.07
Air excess	kmol/hr	0.40	0.61	0.61	0.66	0.77
Gross power	kW	9.84	10.45	11.05	11.63	12.16
Net Power	kW	8.52	9.07	9.62	11.09	10.66
Fuel HHV eff	%	63.90%	67.89%	71.80%	75.57%	79.02%
HB and ST consider	kW	1.21	0.87	0.63	0.56	0.38
Net power Eff (NPE)	%	63.17%	64.59%	66.58%	75.65%	71.75%

3.2 Heat exchanger network (HEN) design

The parametric study shows that at an FU factor of 0.90, the NPE is the highest. In this section, the Aspen Energy Analyzer (AEA) is employed to set up a HEN design for the case with the highest NPE. Also, because of the computational limitations of the AEA, the optimal HEN design provided by AEA is not a Maximum energy recovery network (MERN) design. Because HEN design provided by AEA does not reach the target where only cooling utility is needed, another alternative design by pinch analysis is shown in this section as well to compare the energy savings.

As shown in Figure 6 in the earlier chapter, there are two heater and three coolers required in the process. Fresh air and fuel supplies need to be heated up to the target temperature. The exit gas from the reducer top, the solids from the reducer bottom and the depleted air from the combustor are all at high temperature, where the heat can be recovered for further power generation. After running the simulation, the AEA could read and process the model results and generate existing HEN details including heat duty of each heat exchanger, the area of each heat exchanger, amount of heating and cooling utilities required, utility cost, etc. The detailed results are shown in Table 5 and the HEN diagram is shown in Figure 14.

Heat exchanger details by Aspen Energy Analyzer				
Heat exchanger number	Type	Area (m^2)	Heat duty (KJ/hr)	Heat duty (Gcal/hr)
1 (FCF1HEAT)	Heater	0.3083	2766	6.61E-04
2 (FCA1HEAT)	Heater	4.246	21420	5.12E-03
3 (RGPRE)	Cooler	0.2434	13180	3.15E-03
4 (CGPRE)	Cooler	0.1196	1906	4.56E-04
5 (CAHR)	Cooler	0.7917	18140	4.34E-03
6* (NGSOFC_heat_exchanger)	Cooler	0.1237	47430	1.13E-02
Total utilities			104842	2.51E-02

Table 6: HEN base case details

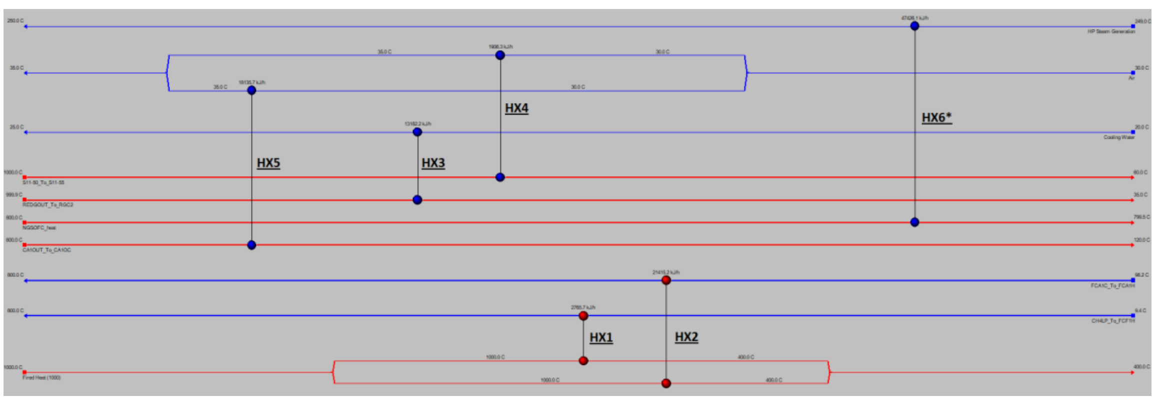

Figure 14: HEN base case diagram generated by AEA

The *DESIGN CHANGE* tool in AEA also offers alternative designs. However, in this case, there is no feasible alternative given by AEA. The U_{min} is the minimum number of heat exchanger needed, which can be calculated by Eq 3.1. $N_{streams}$ is the number of utility type needed. There are five streams involved in this network design. From AEA energy summary, only cooling utility is needed so $N_{utility}$ is 1 and U_{min} is 5. Since the SOFC unit is operated isothermally, a continuous cooling supply is required and the is U_{min} is 6.

$$U_{min} = N_{streams} + N_{utility} - 1 \qquad (16)$$

Figure 15 shows one of the feasible HEN design by pinch analysis with the approach temperature ΔT_{min} of 10 °C. The heat duty of each heat exchanger is labeled in the figure. The new design suggests more than 6 heat exchangers are required. The detailed results can be found in Table 6.

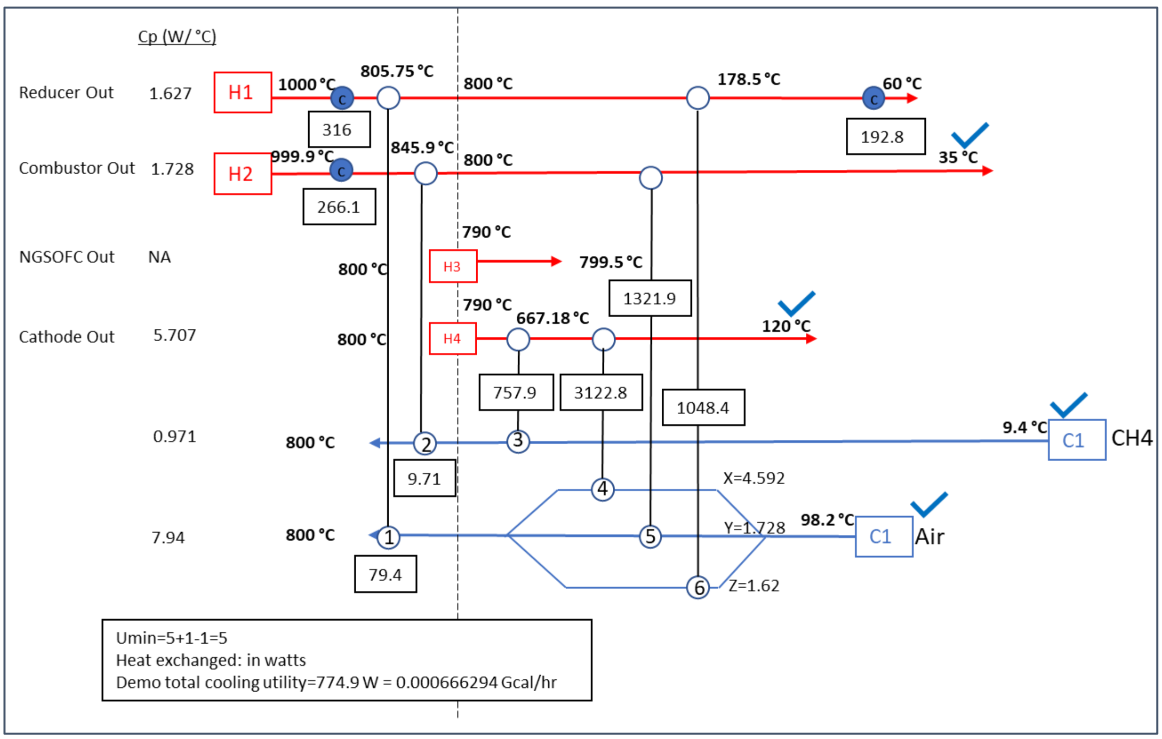

Figure 15: HEN alternative case diagram by manual pinch analysis

Table 7: HEN alternative case details

HEN alternative case by pinch analysis			
Heat exchanger number	Type	Heat duty (Watts)	Heat duty (Gcal/hr)
1	Internal HX	79.4	6.83E-05
2		9.71	8.35E-06
3		757.9	6.52E-04
4		3122.8	2.68E-03
5		1321.9	1.14E-03
6		1048.4	9.01E-04
7	Cooler	316	2.72E-04
8		266.1	2.29E-04
9		192.8	1.66E-04
Total utilities		774.9	6.66E-04

3.3 Energy saving summary

As shown in Table 7, the target heating utilities are 0 which is not met by based case design and the heating utilities are greater than the target value. The heating utility is avoided in alternative design and the total utility is even less than the target value given by AEA. This might be a result of small ΔT_{min} value so the auxiliary utilities are reduced. However, in this case, the total cross-sectional areas are larger than the base case. Furthermore, in the alternative design, an additional 3 heat exchangers are required, which means the fixed cost is higher than the base case design.

Table 8: HEN base case utility summary

Summary Table				
Property	**Actual**	**Target**	**Available Savings**	**% of Actual**
Total Utilities [Gcal/hr]	0.02504	0.01349	0.01	46.13
Heating Utilities [Gcal/hr]	0.005776	0	0.005776	100
Cooling Utilities [Gcal/hr]	0.01926	0.01349	0.00577	29.98
Carbon Emissions [kg/hr]	0	0	0	0

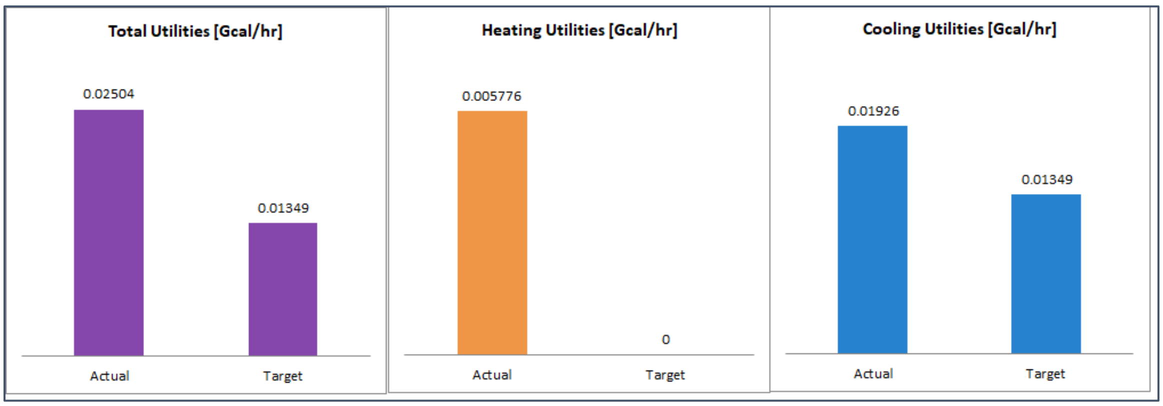

Chapter 4. Conclusions

An Aspen Plus (V10) model is constructed based on specifications of each component of the plant. The parametric studies of FU factor on the plant performance are developed and can be easily extended for studying any potential operating parameters. The simulation results show that the NPE reaches a maximal value of 75.65% when FU is 0.90. The heat balance is considered throughout the study and used for heat integration design. The HEN given by AEA achieves 46.13% energy saving but the numbers of heat exchangers used are equal to $U_{min.}$ Though the HEN alternative design suggests a much lower utility requirement, the cost associated with manufacturing is high.

The simulation results shown in Table 4 suggests that the NPE of an NGSOFC-CLC is higher than that of CLHG-SOFC/GT. According to the efficiencies of some popular power plants with partial or 100% carbon capture as shown in Table 8, the proposed NGSOFC-CLC has significant benefit.

Bibliography

1. B.Fredriksson, M., J.Arriagada, M., & I.Pottsb. (2004). Optimisation of an SOFC/GT system with CO2-capture. *Journal of Power Sources*, 320-326.
2. Doherty, W., Reynolds, A., & Kennedy, D. (2015). Process simulation of biomass gasification integrated with a solid. *Journal of Power Source*, 292-303.
3. EG&G Technical Services, I. (2004). *Fuel Cell Handbook.* Morgantown: U.S. Department of Energy Office of Fossil Energy National Energy Technology Laboratory.
4. EIA. (2018, 02 06). *eia*. Retrieved from www.eia.gov: https://www.eia.gov/outlooks/aeo/pdf/AEO2018.pdf
5. Energy, D. o. (2015). *Cost and Performance Baseline for fossil Energy Plants Volume 1a: Bituminous Coal (PC) and Natural Gas to Electricity Revision3.* U.S. DEPARTMENT OF ENERGY National Energy Technology Laboratory.
6. Fan, L.-S. (2011). *Chemical Looping Systems for Fossil Energy Conversions.* Columbus: John Wiley & Sons, Inc., Hoboken, New Jersey.
7. Nakata, T. &. (2010). Application of energy system models for designing a low-carbon society. *Progress in Energy and Combustion Science*, 462-502.
8. report, D. (2010). *Cost and Performance Baseline for Fossil Energy Plants. Volume 1:*. National Energy Technology Laboratory.

9. Shiyi Chen, Z. X. (2012). An integrated system combining chemical looping hydrogen generation process. *Journal of Power Sources*, 89-98.
10. Tobias Mattisson, A. L. (n.d.). The use of iron oxide as an oxygen carrier in chemical-looping combustion of methane with inherent separation of CO2.
11. W. Zhang a, E. C. (2005). Simulation of a tubular solid oxide fuel cell stack using AspenPlus unit operation models. *Energy Conversion and Management*, 181-196.
12. Yaofan, Y., Ashok, D., Jacob, B., & G. Scott, S. (2005). Fuel flexibility study of an integrated 25 kW SOFC reformer system. *Journal of Power Sources*, 67-76.

Appendix A. Raw data

NG LHV	kJ/kg	47454			CH4 HHV	kJ/kg	55417
NG HHV	kJ/kg	52581			CH4 HHV	kJ/mol	889
NG mass flow	kg/hr	1.000			CH4 mole flow	kmol/hr	0.062
Input	kW	14.606			Fuel	kW	15.393
ST V in 800 C	V	1.037			DC-AC inverter efficiency	%	0.95

		Input	Output
CH4	kmol/hr	0.062	0.003
H2O	kmol/hr	0.000	0.118
CO2	kmol/hr	0.000	0.059
O2 mole frac		0.205	0.09350057
Pressure	bar	1.7	1.7
Temperature	C	800	
FC fuel util		0.95	
FC air utilization		0.6	0.082
Q		0.001	
delta_E	V	-0.079	
Actual E	V	0.958	
Current	A	12696.728	
Gross power (V*I)	kW	12.163	W_sofc*dc
Gross power AC	kw	11.55476	W_sofc*ac
FC fuel comp	kW	0.042	
FC air comp	kW	0.575	W_air*comp
Net power	kW	10.660	
Net efficiency		69.25%	
CO2 compression	kW	0.320328	W_co2*comp
FC total Delta_H	kW	-13.1739	
FC eff_dH base		92.33%	
FC fuel utilization		0.95	
FC eff_fuel HHV base		83.18%	
Cathode gas out	kmol/hr	0.84444	
Combustor gas in	kmol/hr	0.070018	
Excess percent		0.917084	
Cathode Q total	kW	-5.037693	
Cathode Q recoverable	kW	-4.619985	Q_cat